Journal of Marine Research, 49, 203–221, 1991

Tidal stirring and phytoplankton bloom dynamics in an estuary

by James E. Cloern[1]

ABSTRACT

A decade of observation in South San Francisco Bay demonstrates that estuarine phytoplankton biomass fluctuates at the time scale of days to weeks, and that much of this variability is associated with fluctuations in tidal energy. During the spring seasons of every year from 1980–1990, episodic blooms occurred in which phytoplankton biomass rose from a baseline of 2–4 mg chlorophyll *a* m^{-3}, peaked at 20–40 mg chlorophyll *a* m^{-3}, and then returned to baseline values, all within several weeks. Each episode of biomass increase occurred during neap tides, and each bloom decline coincided with spring tides. This suggests that daily variations in the rate of vertical mixing by tidal stirring might control phytoplankton bloom dynamics in some estuaries.

Simulation experiments with a numerical model of phytoplankton population dynamics support this hypothesis. The model incorporates biological processes (light-dependent growth, zooplankton grazing, benthic grazing) and physical processes (sinking, vertical mixing) as controls on the biomass distribution of phytoplankton in a 10-m water column. Numerical simulations indicate that phytoplankton dynamics are highly sensitive to the rate of vertical mixing (parameterized as an eddy diffusivity K_z), such that biomass increases rapidly at small K_z (5 m^2 d^{-1}), but not at large K_z (50 m^2 d^{-1}). Cyclic variation of K_z between 5 and 50 over a 14-d period (simulated neap-spring cycle) yields simulation results that are similar to bloom events observed in this estuary.

1. Introduction

Phytoplankton populations are highly dynamic, and in many environments they experience episodes of rapid biomass increase (blooms), either as recurrent seasonal events or as higher frequency phenomena. Bloom dynamics have been a focus of phytoplankton ecology because: (a) enhanced primary production during blooms influences the energetics and population dynamics of consumer organisms including pelagic and benthic grazers (e.g. Peterson, 1986) as well as bacteria (e.g. Graf *et al.,* 1983; Lancelot and Billen, 1984); (b) large biogeochemical changes can occur in response to blooms, including shifts in the abundance or chemical form of elements such as O, C, N, P, Si, S, Al (e.g. Gordon *et al.,* 1971; Peterson *et al.,* 1985; Turner *et al.,* 1988; Moran and Moore, 1988; Sakamoto and Tanaka, 1989); and (c) blooms of

1. U.S. Geological Survey MS496, 345 Middlefield Road, Menlo Park, California, 94025, U.S.A.

some species can have economic impacts because of degraded water quality or mortality of commercial fish populations (e.g. Underdal *et al.,* 1989).

Although no single mechanism can be invoked to explain blooms, episodes of rapid biomass increase are usually associated with transient physical phenomena (Paerl, 1988), including changes in the rate of vertical mixing as influenced by variations in water column stability. In lakes and the open ocean, such transients result from seasonal fluctuations in the balance between buoyancy inputs from solar heating of the surface layer, and stirring from wind energy. Temperate lakes and open oceans therefore have regular seasonal cycles of altered stability (mixing), and the phytoplankton response to these cycles is usually manifested as blooms during the spring or autumn transitions.

Estuaries are unique aquatic environments that have an additional source of buoyancy input derived from riverine freshwater inflow, and an additional source of mechanical energy input from the tides (tidal stirring). As a consequence of this fundamental physical distinction (Simpson *et al.,* 1990), very different bloom dynamics are observed in estuaries as compared to lakes and the open ocean. In particular, low-frequency variations of estuarine phytoplankton populations can result from seasonal and interannual variations in river flow (e.g. Demers *et al.,* 1986), and high-frequency variations can result from fluctuations in tidal stirring (Sinclair *et al.,* 1981). The purpose of this paper is to describe and analyze bloom dynamics in South San Francisco Bay, an estuary where short-term phytoplankton fluctuations appear to be tightly controlled by tidal variations in vertical mixing. This conclusion is supported by (a) a decade of field observations, and (b) the results of numerical simulation experiments using a model designed to explore mechanisms of bloom dynamics in tidal estuaries.

2. Description of the estuary and methods

a. South San Francisco Bay. South San Francisco Bay (SSFB) is an appendage to the larger San Francisco Bay system, which is the estuary of the Sacramento-San Joaquin Rivers. The South Bay has bathymetric features common to many coastal plain estuaries: a relict river channel (here, 10–15 m deep) that is bounded by subtidal shallows and intertidal mudflats (Fig. 1). The dominant transverse feature is the San Bruno Shoal, which impedes circulation between the South Bay and other basins of the estuary. The hydrology of SSFB is unusual because this estuary receives freshwater inflow from multiple sources. During peak flows of the Sacramento-San Joaquin Rivers, fresh water flows through the northern reach of San Francisco Bay and penetrates across the San Bruno Shoal into South San Francisco Bay. In addition, local runoff from winter storms is delivered to the upper SSFB through smaller creeks (Fig. 1). This configuration leads to complex three-dimensional distributions of salinity (Huzzey *et al.,* 1990), and a dynamic nontidal circulation that is not yet well defined.

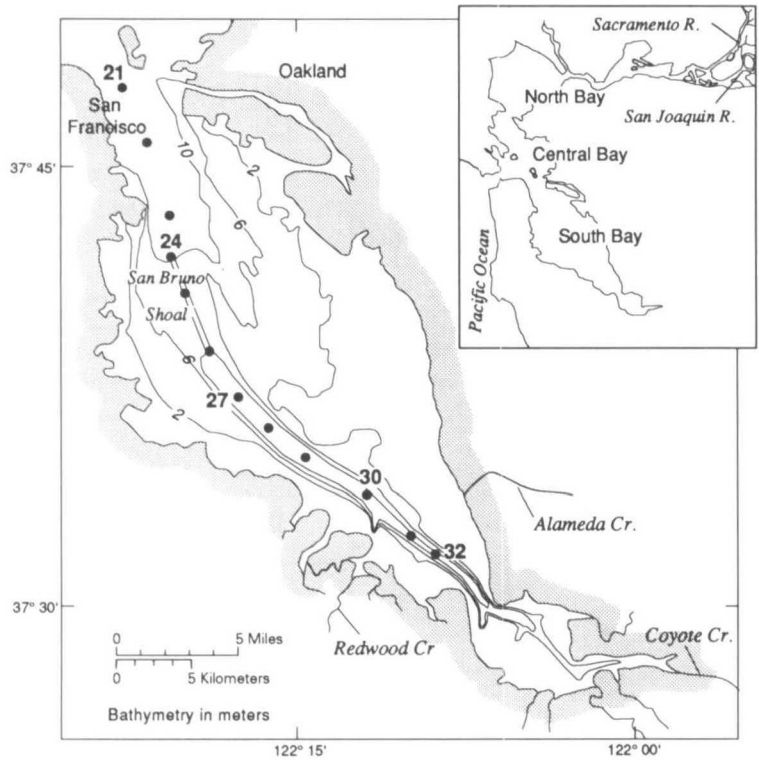

Figure 1. Map of South San Francisco Bay, with sampling sites shown along the deep channel; inset shows location relative to the northern San Francisco Bay estuary and its connection to the Sacramento-San Joaquin Rivers.

The climate of northern California is mediterranean, so SSFB experiences only small seasonal changes in water temperature (typically from 10 to 20°C). However, precipitation and runoff in the river basins are highly seasonal and most freshwater inflow to the estuary occurs during the wet season (approximately December to March). Both local and far-field inputs of fresh water are small during the dry summer-autumn. As a consequence, SSFB has large seasonal fluctuations in salinity and vertical density structure. During the dry season, salinity is spatially uniform and approaches that of seawater; however, during the wet season, there can be sufficient freshwater inflow to depress salinity below 10 and to induce strong salinity and density stratification in the channel.

Winds are also highly seasonal, with maxima (≈ 10 m s^{-1}) associated with winter storms and the diurnal seabreeze in summer (Conomos, 1979). However, the primary input of mechanical energy is from the semidiurnal tides, which have mean amplitude of about 2 m and maximum current speeds in the channel varying between < 0.5 m s^{-1} at neap tides and > 1.0 m s^{-1} at spring tides (Cheng and Gartner, 1985).

Density stratification is highly correlated with tidal current speed, and it fluctuates over the fortnightly (neap-spring) tidal cycle (Cloern, 1984, 1991).

b. Methods. The SSFB estuary has been a site of sustained investigation for over a decade. Although the emphasis, objectives, and scales of study have changed over that time period, a core of hydrographic measurements has been sustained to define the two-dimensional distributions of salinity, temperature, water density, phytoplankton biomass, and turbidity along the SSFB channel. Data presented here were collected at fixed sampling locations, and emphasis is placed on the mid-bay longitudinal transect between stations 24 and 30 (Fig. 1). The period of record is 1980 through spring 1990, when 319 sampling cruises were conducted to map these constituents. Earlier studies (1978–1979) suggested that the most efficient sampling strategy should emphasize the dynamic spring period; beginning in 1980 the SSFB transect was sampled at least once a week during spring, and approximately bimonthly the other seasons. Sampling cruises were not phased with the semidiurnal tides, and recent studies (Cloern *et al.*, 1989; Powell *et al.*, 1989) have quantified variability at the tidal time scale. Because of this variability, the primary quantities of interest here are the mean values of measurements taken along the mid-bay transect, which is approximately twice the length of the tidal excursion.

Prior to 1987, sampling was done by pumping seawater from discrete depths to instruments aboard ship (an inductive salinometer, thermistor, and Turner Designs Model 10 fluorometer). Profiles were usually obtained at only five sites (numbered stations, Fig. 1), and they provided vertical resolution of about 2–4 m. Water transparency was measured with a Secchi disk or from vertical profiles of irradiance measured with a LiCor 192S quantum sensor. Beginning in 1987, sampling was done with a Seabird SBE9/11 CTD, Sea Tech *in-situ* fluorometer, and LiCor 192S quantum sensor. This instrument package was deployed at all 12 stations, and was configured to take vertical measurements approximately every 2 cm. Data presented here are mean values centered around one-meter increments from every vertical profile.

The fluorometers were calibrated each cruise with 6–12 discrete measures of chlorophyll *a* concentration. Water samples were taken with a Niskin bottle, or from the shipboard fluorometer outlet, and collected onto Gelman A/E filters. Chlorophyll *a* concentration was determined spectrophotometrically using the methods described in Strickland and Parsons (1972), and the phaeopigment correction was done according to Lorenzen (1967). Results presented here are calculated chlorophyll *a* concentrations from the fluorometer measurements; these values typically deviated from the discrete chlorophyll measurements by less than 10%. Detailed sampling methods are presented in data reports (e.g. Wienke *et al.*, 1990).

For the period 1978–1983, phytoplankton populations were also examined microscopically to determine taxonomic composition and to estimate biomass independently of the chlorophyll *a* measurements (e.g. Wong and Cloern, 1982). Samples

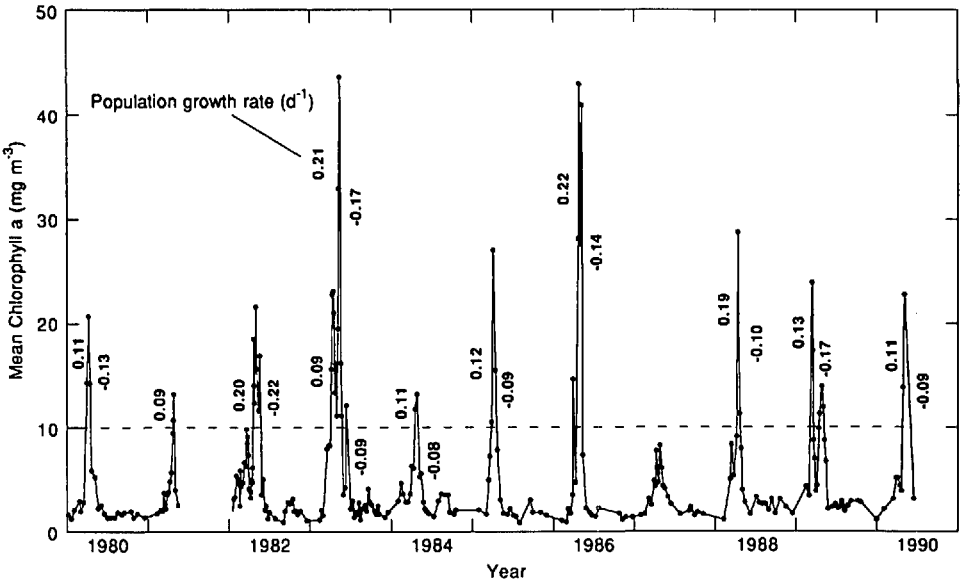

Figure 2. Phytoplankton biomass in South San Francisco Bay, January 1980 through May 1990; values are mean chlorophyll *a* concentration in the euphotic zone along the mid-bay transect (stations 24–30, Fig. 1). Also shown are net population growth rates *R*, from Eq. 1.

were preserved in an acidic Lugol solution and examined at both 100x and 1000x using an inverted microscope. Algal biovolume was determined from cell dimensions measured with an ocular micrometer, and biomass as carbon from the empirical equations of Strathmann (1967).

In addition to the core measurements, other specific programs were conducted during this period to characterize: primary productivity (Cole and Cloern, 1984, 1987), phytoplankton population growth rates (Alpine and Cloern, 1988), lateral variability across the shallows (Powell *et al.*, 1989; Huzzey *et al.*, 1990), the phytoplankton component of seston (Wienke and Cloern, 1987), small-scale spatial variability (Powell *et al.*, 1986), phytoplankton size distributions (Cole *et al.*, 1986), significance of light limitation (Cloern, 1987), phytoplankton responses to stratification dynamics (Cloern, 1984), and seasonal population budgets for phytoplankton of SSFB (Cloern, 1982).

3. Phytoplankton biomass variability: A decade of observation

a. Seasonal variability. For the period 1980–1990, phytoplankton biomass along the SSFB channel was consistently low except for short episodes of rapid increase that occurred in spring (usually March or April). Although the duration and magnitude of the spring bloom varied among years, it was a persistent feature that occurred every year of the decade (Fig. 2). Based on those periods when samples were examined

microscopically, the episodes of chlorophyll increase were also episodes of increasing phytoplankton cell number and biovolume. For example, during spring months of 1980–1983 phytoplankton abundance often exceeded 50×10^6 cells liter^{-1} (estimated biomass > 2.5 mg C liter^{-1}). However during summer-autumn, cell abundance was typically of the order 2–5 $\times$ 10^6 cells liter^{-1} (0.1 to 0.5 mg C liter^{-1}). Hence the time series of chlorophyll *a* concentration shown in Figure 2 reflects changes in phytoplankton biomass over the decade. Size-fractionation of chlorophyll indicated that the spring blooms were composed primarily of nanoplankton (<20 μm; Cole *et al.*, 1986). This was confirmed with microscopy: spring blooms were dominated typically by assemblages of pigmented microflagellates (cryptophytes, haptophytes, naked dinoflagellates), and small centric diatoms (*Thalassiosira* spp., *Cyclotella* spp., *Skeletonema costatum*). The phototrophic ciliate *Mesodinium rubrum* was also abundant during the largest blooms.

The occurrence of blooms only during spring is presumably a consequence of the enhanced water column stability that occurs following freshwater inflow during the wet season. Water column stability can promote blooms by inhibiting vertical mixing, such that phytoplankton biomass is produced in the euphotic zone faster than it is transported to the lower aphotic layer (e.g. Sinclair, 1978) or to benthic consumers (e.g. Daborn, 1986). One index of stability is the mean vertical density gradient, calculated here as the difference ($\Delta\sigma_t$) between sigma-*t* measured at 10-m depth and the surface. Density stratification was highly dynamic but strongest during the spring when most measures of $\Delta\sigma_t$ ranged between 0.1 and 1.1 kg m^{-3} (Fig. 3). However, density stratification was weak throughout the dry summers and autumns, when most measures of $\Delta\sigma_t$ were <0.2 kg m^{-3} (median $\Delta\sigma_t$ = 0.08).

The spring seasons were also periods of high and variable phytoplankton biomass (Fig. 3). Chlorophyll *a* concentrations typically fell in the range of 3 to 9 mg m^{-3} during spring, and exceeded 10 mg m^{-3} only during this season (Fig. 2). On the other hand, phytoplankton biomass was typically less than 2 mg chlorophyll *a* m^{-3} during the dry summer-autumn. Seasonal variability of phytoplankton biomass was therefore associated with changes in density stratification that resulted from the strong seasonality of freshwater (i.e., buoyancy) input to the estuary. This association holds at the interannual time scale as well. For example, years of heavy precipitation and runoff, such as 1983 and 1986, were the years of most intense density stratification and most persistent spring blooms (Cloern, 1991).

These observations establish a strong connection between phytoplankton dynamics and hydrology at long time scales: runoff during the wet seasons and years establishes a physical regime that is conducive to bloom formation. However, this connection does not hold at the shorter time scale associated with the daily evolution of individual bloom events. At this shorter time scale there was no correlation between phytoplankton biomass and either river flow or density stratification. What, then, controls the short-term dynamics of phytoplankton populations including the inception, magnitude, and duration of blooms during the spring?

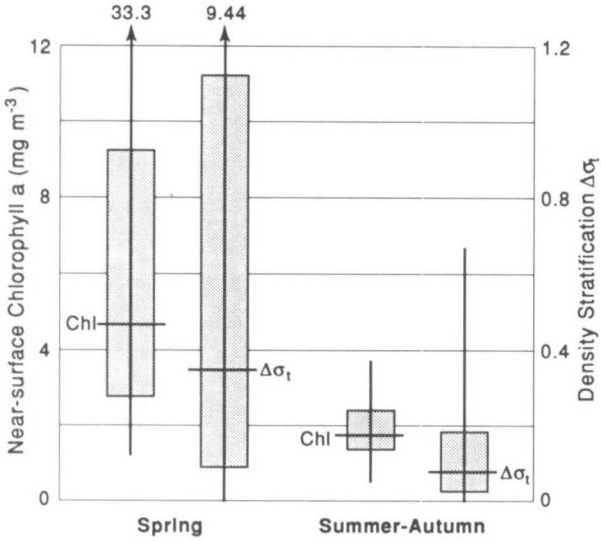

Figure 3. Box plots showing seasonal changes in phytoplankton biomass (near-surface chlorophyll *a* concentration) and density stratification ($\Delta\sigma_t$) at sites along the SSFB channel during the period 1980–1990. The spring season includes all measurements made from 15 February to 15 May (n = 275); summer-autumn includes all measurements made from 15 July to 15 October (n = 122). Box plots show the median, quartiles (boxes), and upper/lower 5th percentiles of all measurements.

b. Daily-weekly variability. Observations in SSFB (Cloern, 1984), as in other tidal estuaries (e.g. Winter *et al.,* 1975; Sinclair, 1978; Haas *et al.,* 1981), have shown that rapid phytoplankton population growth often occurs during periods of low tidal energy (neap tides). This suggests that biomass variability at shorter time scales might be regulated by tidal stirring, and that observed biomass changes should therefore be correlated with tidal current speed. To test this hypothesis, I calculated the net growth rate of phytoplankton populations for each bloom event observed in SSFB during 1980–1990, using:

$$R = \ln [B_j/B_{j-1}]/\Delta t, \tag{1}$$

where B_j is mean near-surface chlorophyll *a* concentration along the mid-bay transect on date j, and Δt is the time interval between sampling dates j-1 and j (usually about a week). Changes of R are shown in Figure 2 for events when B exceeded 10 mg chlorophyll *a* m^{-3} (an arbitrary definition of blooms).

Every bloom observed during 1980–1990 was characterized by a net population growth rate of about 0.1 to 0.25 d^{-1} (doubling time <3 to 7 d); bloom declines occurred at comparable rates. Figure 4 shows that for the 12 distinct events observed this decade, there was a significant correlation between population growth rate R and u_7, the seven-day running mean of maximum daily predicted current speed at the mouth of San Francisco Bay (e.g. NOAA, 1982). (It should be noted that significant

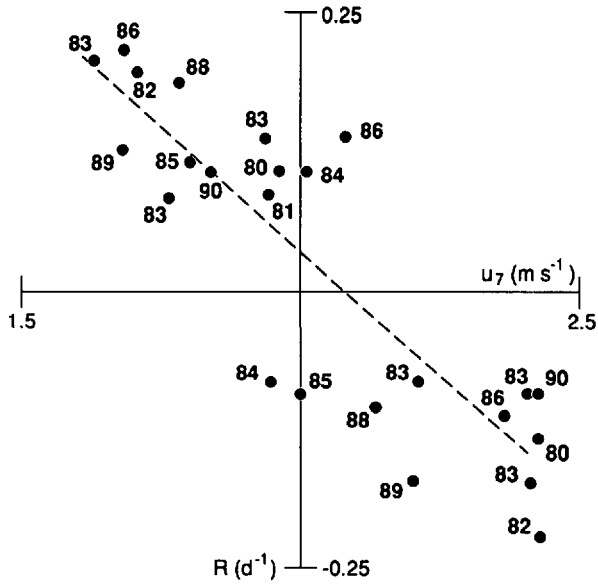

Figure 4. Net rates of biomass increase/decrease R (Eq. 1) for each spring bloom observed in SSFB 1980–1990, against maximum current speed. u_7 is the daily maximum current speed, predicted at the entrance to San Francisco Bay (e.g. NOAA, 1982), averaged over the week preceding each sampling date. Data labels show the year of each bloom. ($r = -0.87$, significant at $P < 0.05$).

correlations also exist for other averaging periods and other indices of tidal energy such as u_7^3, an index of the dissipation rate of tidal kinetic energy.) This relation shows that phytoplankton blooms (large, positive R) always occurred during sustained weak tides ($u_7 < 1.8$ m s^{-1}), and that bloom declines (negative R) always followed periods of strong tidal currents ($u_7 > 2.2$ m s^{-1}). Hence at the daily-weekly time scale, phytoplankton bloom dynamics in SSFB appear to be strongly correlated with changes in tidal energy.

c. Spatial variability. Phytoplankton biomass in SSFB exhibits variability at small spatial scales (Powell *et al.,* 1986), and over the tidal time scale (Cloern *et al.,* 1989). However, the coarse-scale spatial distribution of biomass during blooms often followed the patterns shown in Figure 5, with biomass increasing upestuary, and most notably above the San Bruno Shoal. Powell *et al.* (1986) inferred that this topographic feature partitions SSFB into a seaward regime that is closely connected to the coastal ocean, and a landward regime having slow exchange with the coastal ocean. Horizontal distributions of phytoplankton biomass (Fig. 5) were consistent with this inference and suggest that blooms are the result of *in-situ* production rather than longitudinal advection of biomass. Spring blooms were often characterized by large vertical gradients, especially during strong density stratification when near-

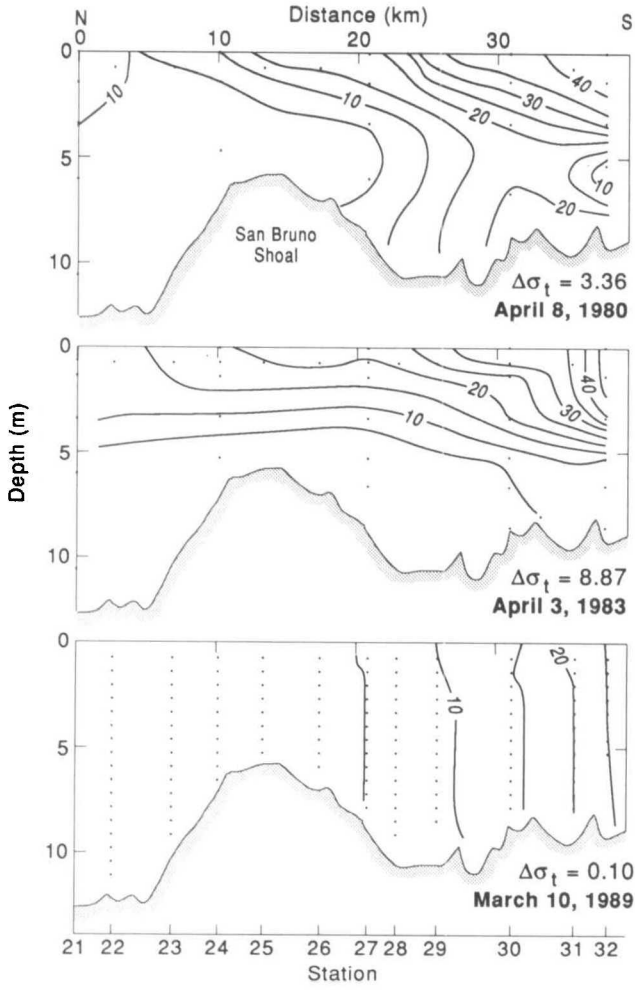

Figure 5. Representative distributions of phytoplankton biomass (chlorophyll *a* concentration, mg m^{-3}) along the SSFB channel during spring blooms occurring at three levels of density stratification ($\Delta\sigma_t$ here is the mean density gradient calculated at all stations where profiles were obtained).

surface chlorophyll concentrations were 2–5 times higher than those below the pycnocline (Fig. 5). Such rapid growth of biomass above the pycnocline is a typical feature of bloom dynamics in estuaries that undergo episodic stratification, such as Puget Sound (Winter *et al.,* 1975), the lower St. Lawrence estuary (Sinclair, 1978), York River estuary (Haas *et al.,* 1981), Long Island Sound (Peterson, 1986), and the Gernika estuary (Bay of Biscay; de Madariaga *et al.,* 1989). Spring blooms occurred in SSFB even during dry years of weak stratification (e.g. 1989), but these were typically of smaller magnitude or duration and characterized by smaller vertical gradients of biomass.

4. Vertical mixing and blooms: A modeling analysis

The observations described above suggest the following two propositions that may apply to estuaries such as SSFB, where density stratification changes over interannual, seasonal, and daily-weekly time scales:

Proposition #1: Vertical mixing in some estuaries is controlled largely by the balance between (a) buoyancy input from freshwater inflow, which varies over long time scales (seasons, years), and (b) the dissipation of tidal kinetic energy, which varies over shorter time scales (e.g. days).

Proposition #2: Phytoplankton population dynamics in these estuaries are strongly influenced by daily fluctuations in vertical mixing. Blooms occur when vertical mixing is maintained at a "slow" rate (to be defined) for a sufficient duration to allow for biomass increase.

Both of these propositions can be explored with modeling analyses, and the purpose here is to present results of numerical simulation experiments using a model that was developed to address this second proposition above (proposition #1 has been addressed with modeling analyses by Simpson *et al.,* 1990). This is a deterministic, rational, and explanatory model (Platt *et al.,* 1977) that was developed specifically to answer the following questions: (1) Are estuarine phytoplankton populations sensitive to daily fluctuations in vertical mixing by tidal stirring? and, (2) What mechanisms allow for blooms to grow and then disappear within a period of weeks? The model evolved from the following general considerations and assumptions:

a. the dynamic quantity of interest (dependent variable) is phytoplankton biomass, measured as chlorophyll concentration.

b. the time scale of interest is days, and particularly the daily evolution of blooms over the neap-spring period; phenomena with shorter time scales (photoperiod, diel rhythms, semidiurnal tides; e.g. Demers *et al.,* 1986) are not considered.

c. the spatial domain of interest is the vertical dimension, because vertical gradients of phytoplankton biomass can greatly exceed horizontal gradients during blooms (Fig. 5); horizontal transports may play a role in the evolution of blooms (see Huzzey *et al.,* 1990), but they are excluded from the analysis presented here.

d. vertical mixing results primarily from tidal stirring, and it can be parameterized as an eddy diffusivity; the daily mean diffusivity scales with the maximum daily tidal current speed (see Winter *et al.,* 1975); as a first approximation, the eddy diffusivity is spatially uniform.

e. phytoplankton population growth rate is limited by the availability of light energy, but not by nutrient availability (Cloern, 1991); light attenuation derives primarily from scattering/absorption by suspended mineral particles.

f. phytoplankton biomass is lost in the water column to respiration and zooplankton grazing, and at the bed to grazing by benthic infauna; these processes can be approximated as first order losses.

g. phytoplankton transports result from sinking and vertical mixing.

Table 1. Variable names and their values used in the estuarine phytoplankton model.

Name	Value	Units	Description
$B(t,z)$		mg m^{-3}	Phytoplankton Biomass (chl *a*)
z		m	Depth
t		d	Time
$\mu(z)$		d^{-1}	Phytoplankton Growth Rate
r	0.1	d^{-1}	Phytoplankton Respiration Rate
G	0.1	d^{-1}	Zooplankton Grazing Rate
$I(0)$	40	Einst. m^{-2} d^{-1}	Incident Solar Radiation (PAR)
k	1.3	m^{-1}	Light Attenuation Coefficient
K_z	5-50	m^2 d^{-1}	Vertical Eddy Diffusivity
w_s	0.5	m d^{-1}	Phytoplankton Sinking Rate
α	8	m^3 m^{-2} d^{-1}	Benthic Grazing Rate
H	10	m	Water Column Height

a. Mathematical model. The conceptual model above can be formalized as a differential equation to define the time (t)- and depth (z)-dependent rate of biomass change:

$$\frac{\partial B}{\partial t} = (\mu - r)B - GB - \frac{\partial}{\partial z}(w_s B) + \frac{\partial}{\partial z}(K_z\, \partial B/\partial z), \tag{2}$$

where B is phytoplankton biomass as chlorophyll *a* concentration; μ is light-dependent specific growth rate; r is specific respiration rate; G is the loss rate to zooplankton grazing; w_s is sinking speed of phytoplankton; and K_z is the vertical eddy diffusivity (all units are given in Table 1). In the numerical experiments described below, all parameters (except K_z) were held at constant values chosen to approximate the biological/physical conditions of South San Francisco Bay during spring.

The phytoplankton growth rate was calculated from measures of productivity P (mg C mg^{-1} chl *a* d^{-1}), which fit the hyperbolic tangent function of Jassby and Platt (1976):

$$P(z) = P_{max}[\tanh |aI(z)| - r], \tag{3}$$

where $P(z)$ is the biomass-specific rate of photosynthesis at depth z; P_{max} is the light-saturated rate of photosynthesis; a defines photosynthetic efficiency at low irradiance; $I(z)$ is irradiance at depth z; and r is the respiration rate. Based on numerous measures of productivity in SSFB (Cole and Cloern 1984, 1987), the three parameters of Eq. 3 were chosen as: P_{max} = 100 mg C mg^{-1} chl *a* d^{-1}; a = 0.1; and r = 0.05 (i.e., respiration loss is five percent of the maximum photosynthetic rate P_{max}). The depth distribution of photosynthetically active radiation is given by:

$$I(z) = I(0)\exp(-kz), \tag{4}$$

where $I(0)$ is mean daily surface irradiance (= 40 Einsteins m^{-2} d^{-1}) and k is the mean light attenuation coefficient (= 1.3 m^{-1}) in SSFB during spring. Assuming that

the ratio of phytoplankton cellular carbon to chlorophyll *a* (θ) is a constant value of 50 (Wienke and Cloern, 1987), then productivity can be converted into specific growth rate μ:

$$\mu(z) = P(z) \div \theta \tag{5}$$

$$= 100[\tanh\{0.1 \times 40 \exp(-1.3\, z)\} - 0.05] \div 50 \tag{6}$$

$$= 2[\tanh\{4 \exp(-1.3\, z)\} - 0.05]. \tag{7}$$

Grazing has been estimated previously (Cloern, 1982) from measured abundances of selected categories of zooplankton (life history stages of copepods, tintinnid ciliates, meroplankton) and published empirical formulations relating ingestion rate to body size. This analysis indicated that the macrozooplankton graze about ten percent of phytoplankton biomass daily, so the parameter G was fixed at 0.1 d^{-1}; no consideration, as yet, has been given to microzooplankton grazing in this estuary. The phytoplankton sinking speed w_s was fixed at 0.5 m d^{-1}, a relatively slow speed consistent with measurements made on other nanoplankton-dominated communities (e.g. Riebesell, 1989).

The surface boundary condition was treated in a standard manner (e.g. Winter *et al.,* 1975; Jamart *et al.,* 1977) by specifying zero phytoplankton flux at the air-water interface:

$$K_z \frac{\partial B}{\partial z} - w_s B = 0; (z = 0). \tag{8}$$

Benthic grazing was incorporated in the model as the bottom boundary condition, in which the flux of phytoplankton biomass was set equal to a grazing rate α, times biomass at the bed (water depth H = 10 m):

$$K_z \frac{\partial B}{\partial z} - w_s B = -\alpha B; (z = H). \tag{9}$$

The benthic grazing rate α was fixed at 8 $m^3\, m^{-2}\, d^{-1}$, a value consistent with measured abundances of benthic macrofauna in SSFB and calculated rates of filtration by the most abundant taxa (Cloern, 1982).

These biological and physical processes are represented in Figure 6, which shows the depth distribution of net population growth rate in a well-mixed 10-m water column. Note that the net compensation depth [where $(\mu - r - G) = 0$] occurs at about 3 m. Therefore, the upper 30% of the water column is a source of phytoplankton biomass, whereas the lower 70% is a sink for biomass resulting from losses to respiration and zooplankton grazing. A further loss is localized at the bed, at a rate proportional to the vertical flux of biomass there. This treatment of biological processes remained fixed for all simulation experiments. However, the vertical mixing rate (eddy diffusivity K_z) was changed between simulations as an approach toward answering the questions posed above.

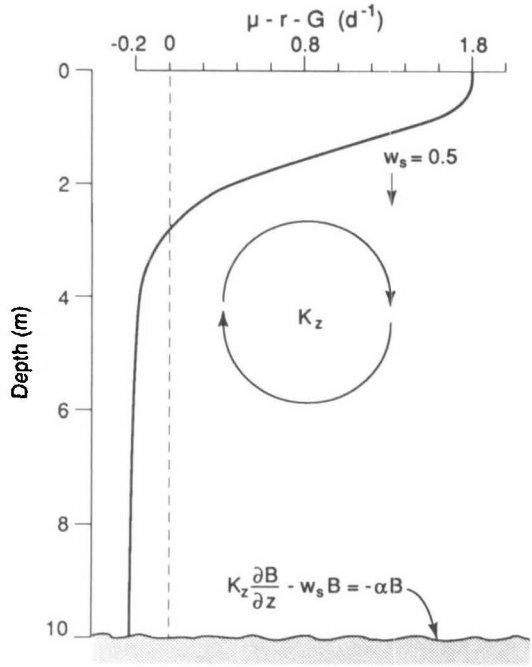

Figure 6. Schematic of the estuarine phytoplankton model, showing depth distribution of net growth rate (Eq. 7). Sinking and turbulent diffusion transport phytoplankton biomass from the upper trophogenic zone to the lower aphotic zone and bed, where biomass is consumed.

Eq. 2 was solved numerically using the implicit Crank-Nicolson finite-difference method (Ames, 1977). All simulations were done for 14 d, representing one neap-spring tidal period, using a time step of 0.002 d. A fixed grid spacing of 0.01 m was found to yield stable and accurate results. The initial condition was specified as a uniform biomass B of 3 mg chlorophyll *a* m^{-3} throughout the water column (i.e., "prebloom" condition).

b. Numerical experiments. Model results are shown below for three physical conditions: Case 1 = constant slow vertical mixing (K_z = 5 m^2 d^{-1}); Case 2 = constant rapid vertical mixing (K_z = 50 m^2 d^{-1}); and Case 3 = simulated neap-spring cycle in which K_z varied periodically over 14-d. Although eddy diffusivities have not been measured explicitly in SSFB, these values fall within the large range of depth- and tidally-averaged values of K_z estimated for other stratified or partially stratified estuaries (see, e.g., the review by Officer, 1977).

For the Case 1 condition of slow vertical mixing, simulated phytoplankton biomass increased continually over the 14-d period, producing high biomass and strong vertical gradients (Fig. 7a). This simulated bloom is a consequence of rapid population growth in the euphotic zone, coupled with slow vertical transports (sinking, diffusion) from the upper water column to the lower water column and bed where

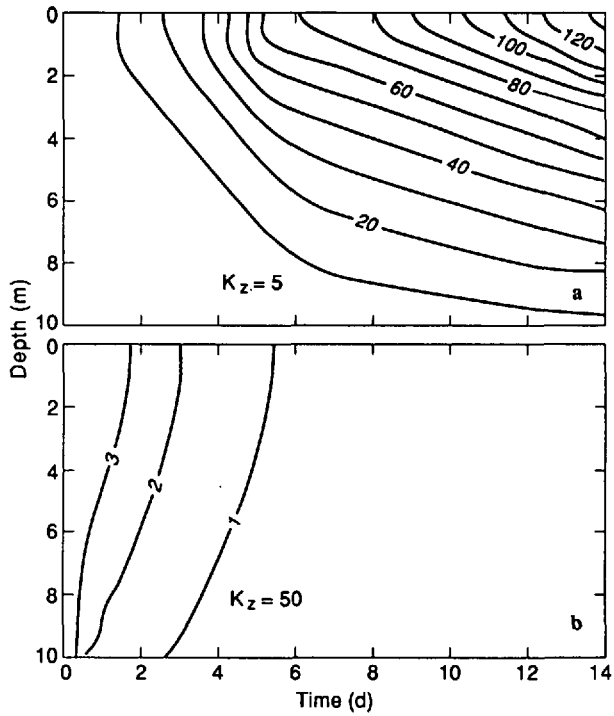

Figure 7. Simulated phytoplankton biomass for conditions of (a) constant slow vertical mixing (K_z = 5 m^2 d^{-1}) and (b) constant rapid vertical mixing (K_z = 50 m^2 d^{-1}). Isopleths show depth distribution of chlorophyll *a* concentration over simulation periods of 14 d. Note difference in contour intervals between the two simulations.

consumption occurs. Hence under conditions of slow mixing (small K_z), the vertical distribution of the source term [$\mu(z)$] dominates the vertical distribution of biomass; net population growth can occur because the depth-averaged value of $\mu(z)$ is positive (production > water column consumption), and because transport to the benthos is slow. This general result is reminiscent of observations made in numerous estuaries, where surface blooms occur in response to enhanced density stratification and, therefore, reduced vertical mixing (e.g., Winter *et al.*, 1975; Sinclair, 1978; Haas *et al.*, 1981; Ingram *et al.*, 1985; Peterson, 1986; de Madariaga *et al.*, 1989).

For the Case 2 condition of rapid vertical mixing, biomass declined continually over the 14-d simulation period (Fig. 7b). This outcome is a consequence of the enhanced vertical flux of biomass from the water column to the bed [large value of $K_z \partial B/\partial z$], which exceeded net production in the overlying water column. In this case, the vertical distribution of biomass is dominated by diffusive transport, and biomass declines because of rapid transport to benthic grazers. This numerical result is consistent with speculations (e.g. Daborn, 1986) that increased vertical mixing enhances the coupling between phytoplankton and benthic consumers in estuaries.

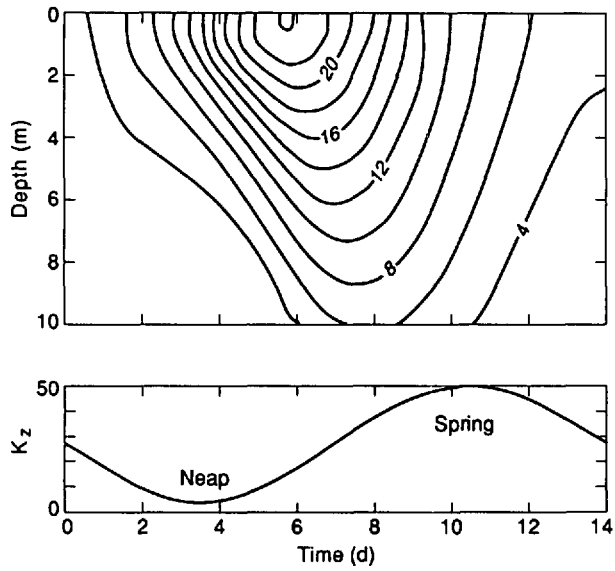

Figure 8. Simulated phytoplankton biomass for time-variable vertical diffusivity (bottom panel), approximating a neap-spring cycle. Upper panel shows depth distribution of chlorophyll *a* concentration calculated for the 14-d period.

The contrasts between simulation results of Case 1 and Case 2 are striking, and indicate that only a ten-fold change in the vertical eddy diffusivity can greatly influence phytoplankton dynamics in a tidal estuary where benthic grazing occurs. We can calculate a time scale τ for vertical mixing as $0.4H^2/K_z$, the time required for a passive tracer at the surface to mix uniformly over water depth H (Fischer *et al.*, 1979). For the Case 1 condition above, $\tau = 8$ d; and for Case 2, $\tau = 0.8$ d. Hence with the biological kinetics (of growth, sinking, benthic grazing) chosen here to represent SSFB, phytoplankton biomass increases (a bloom occurs) when the time scale of vertical mixing is on the order of a week. However, blooms can not develop when the time scale of vertical mixing is a day or less.

With these results in mind, the Case 3 condition was simulated as a first-order approximation to the daily variation in tidal stirring that occurs over a neap-spring cycle. It is based on observations that K_z varies over the neap-spring period in estuaries (e.g. Bowden, 1963), and empirical formulations that scale K_z with current speed (e.g. Bowden and Hamilton, 1975). Case 3 is presented in Figure 8, which shows the periodic variation of K_z between a minimum value of 5 (simulated neap tide) and a maximum value of 50 $m^2 d^{-1}$ (simulated spring tide). Simulated phytoplankton biomass increased almost ten-fold in the surface layer during the 1 wk period of slow vertical mixing; strong vertical gradients occurred during this simulated neap tide; and biomass peaked about 2-3 d after the K_z minimum. However, as K_z then increased to 50, the simulated biomass declined and became more uniformly

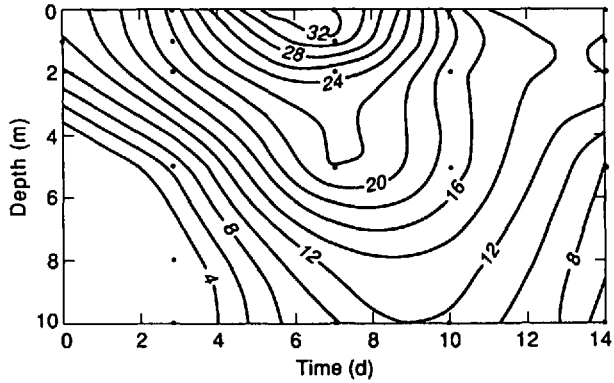

Figure 9. Measured depth distributions of chlorophyll *a* in mid-SSFB (station 27, Fig. 1), during the spring bloom of 5–19 April 1983.

distributed. After the spring tide period of enhanced vertical mixing (day 14), biomass distribution was similar to the initial condition. Although this numerical model is a gross oversimplification, it produces simulations that are remarkably similar to bloom events during periods of low tidal energy and strong stratification in SSFB. As an example, Figure 9 shows the evolution of one bloom that occurred around a neap tide during April 1983. These simulation results are consistent with the hypothesis that phytoplankton population dynamics can be regulated by daily changes in vertical mixing by tidal stirring.

The modeling analysis presented here is based on simplistic approximations that were invoked to answer one narrow set of questions about the connections between vertical mixing and phytoplankton populations. Other mechanisms of estuarine phytoplankton variability can be pursued with future refinements of the model described here, including: (a) horizontal advection (by extending the model to two spatial dimensions); (b) tidal resuspension and short-term fluctuations in light attenuation (by specifying k as a function of current speed; e.g. Cloern *et al.,* 1989); and (c) spatial variability of K_z (as a function of tidal shear and the vertical density gradient).

5. Concluding comments

A decade of observation in South San Francisco Bay confirms that variability over periods of days to weeks is an important component of phytoplankton population dynamics in estuaries. These observations, plus simulation results, suggest the following:

1. For nutrient-rich estuaries, at least, much of the temporal variability of phytoplankton biomass (and production) is driven by variability of physical forcings that influence vertical mixing.

2. Different physical forcings apparently influence phytoplankton populations at different time scales. For example, in estuaries such as SSFB, where vertical mixing is

largely controlled by the balance between buoyancy inputs from river flow and stirring by tides, phytoplankton populations change over the dominant time scales of variability of both river flow (e.g. seasons) and the tides (e.g. days).

3. Estuaries are physical environments distinct from lakes and the open ocean, where surface heating and wind stirring determine the vertical energy balance. Therefore, we might expect variance spectra of phytoplankton biomass in estuaries to have a different character from those in lakes and the ocean.

4. However, just as in lakes and the ocean, a problem of critical biological and biogeochemical importance in estuaries is the characterization of turbulent mixing. Realistic simulation of phytoplankton populations, and other dynamic properties, is dependent upon accurate descriptions of mixing processes in estuaries, including the identification of mechanisms and time scales of vertical mixing.

Acknowledgments. The data set presented here is a result of the diligent work of my colleagues Andrea Alpine, Brian Cole and Sally Wienke, and the recognition by USGS managers of the need for long-term programs of basic research. Jeff Koseff, Steve Monismith, Jackie Holen, and Ralph Cheng all provided valuable guidance in model development. I also thank Jeff Koseff, Ken Bencala and two anonymous reviewers for their thoughtful evaluations of an earlier version of this paper.

REFERENCES

Alpine, A. E. and J. E. Cloern. 1988. Phytoplankton growth rates in a light-limited environment, San Francisco Bay. Mar. Ecol. Progr. Ser., *44,* 167–173.

Ames, W. F. 1977. Numerical Methods for Partial Differential Equations, New York, Academic.

Bowden, K. F. 1963. The mixing processes in a tidal estuary. Internat. J. Air Water Pollut., *7,* 343–356.

Bowden, K. F. and P. Hamilton. 1975. Some experiments with a numerical model of circulation and mixing in a tidal estuary. Est. Coast. Mar. Sci., *3,* 281.

Cheng, R. T. and J. W. Gartner. 1985. Harmonic analysis of tides and tidal currents in South San Francisco Bay, California. Est. Coast. Shelf Sci., *21,* 57–74.

Cloern, J. E. 1982. Does the benthos control phytoplankton biomass in South San Francisco Bay (USA)? Mar. Ecol. Progr. Ser., *9,* 191–202.

—— 1984. Temporal dynamics and ecological significance of salinity stratification in an estuary. Oceanol. Acta, *7,* 137–141.

—— 1987. Turbidity as a control on phytoplankton biomass and productivity in estuaries. Cont. Shelf Res., *7,* 1367–1381.

—— 1991. Annual variations in river flow and primary production in the South San Francisco Bay Estuary, *in* Estuaries and Coasts: Spatial and Temporal Intercomparisons, Elliott, M. and D. Ducrotoy, eds., Fredensborg, Denmark, Olsen and Olsen.

Cloern, J. E., T. M. Powell and L. M. Huzzey. 1989. Spatial and temporal variability in South San Francisco Bay. II. Temporal changes in salinity, suspended sediments, and phytoplankton biomass and productivity over tidal time scales. Est. Coast. Shelf Sci., *28,* 599–613.

Cole, B. E. and J. E. Cloern. 1984. Significance of biomass and light availability to phytoplankton productivity in San Francisco Bay. Mar. Ecol. Progr. Ser., *15,* 15–24.

—— 1987. An empirical model of phytoplankton productivity in estuaries. Mar. Ecol. Progr. Ser., *36,* 299–305.

Cole, B. E., J. E. Cloern and A. E. Alpine. 1986. Biomass and productivity of three phytoplankton size classes in San Francisco Bay. Estuaries, *9,* 117–126.

Conomos, T. J. 1979. Properties and circulation of San Francisco Bay waters, *in* San Francisco Bay: The Urbanized Estuary, T. J. Conomos, ed., San Francisco, Pacif. Div. Am. Assoc. Adv. Sci., 47–84.

Daborn, G. R. 1986. Effects of tidal mixing on the plankton and benthos of estuarine regions of the Bay of Fundy, *in* Tidal Mixing and Plankton Dynamics, M. J. Bowman, C. M. Yentsch and W. T. Peterson, eds., New York, Springer-Verlag, 390–413.

Demers, S., L. Legendre and J.-C. Therriault. 1986. Phytoplankton responses to vertical tidal mixing, *in* Tidal Mixing and Plankton Dynamics, M. J. Bowman, C. M. Yentsch and W. T. Peterson, eds., New York, Springer-Verlag, 1–40.

Fischer, H. B., E. J. List, R. C. Y. Koh, J. Imberger and N. H. Brooks. 1979. Mixing in Inland and Coastal Waters, New York, Academic.

Gordon, L. I., P. K. Park, S. W. Hager and T. R. Parsons. 1971. Carbon dioxide partial pressures in north Pacific surface waters—time variations. J. Oceanogr. Soc. Japan, *27,* 81–90.

Graf, G., R. Schulz, R. Peinert and L.-A. Meyer-Reil. 1983. Benthic response to sedimentation events during autumn to spring at a shallow-water station in the Western Kiel Bight. I. Analysis of processes on a community level. Mar. Biol., *77,* 235–246.

Haas, L. W., S. J. Hastings and K. L. Webb. 1981. Phytoplankton responses to a stratification-mixing cycle in the York River estuary during late summer, *in* Estuaries and Nutrients, B. J. Neilson and L. E. Cronin, eds., Clifton, N. J., Humana, 619–636.

Huzzey, L. M., J. E. Cloern and T. M. Powell. 1990. Episodic changes in lateral transport and phytoplankton distribution in South San Francisco Bay. Limnol. Oceanogr., *35,* 472–478.

Ingram, R. G., L. Legendre, Y. Simard and S. Lepage. 1985. Phytoplankton response to freshwater runoff: the diversion of the Estmain River, James Bay. Can. J. Fish. Aquat. Sci., *42,* 1216–1221.

Jamart, B. M., D. F. Winter, K. Banse, G. C. Anderson and R. K. Lam. 1977. A theoretical study of phytoplankton growth and nutrient distribution in the Pacific Ocean off the northwestern U.S. coast. Deep-Sea Res., *24,* 753–773.

Jassby, A. D. and T. Platt. 1976. Mathematical formulation of the relationship between photosynthesis and light for phytoplankton. Limnol. Oceanogr., *21,* 540–547.

Lancelot, C. and G. Billen. 1984. Activity of heterotrophic bacteria and its coupling to primary production during the spring phytoplankton bloom in the southern bight of the North Sea. Limnol. Oceanogr., *29,* 721–730.

Lorenzen, C. J. 1967. Determination of chlorophyll and phaeopigments: spectrophotometric equations. Limnol. Oceanogr., *12,* 343–346.

de Madariaga, I., E. Orive and G. T. Boalch. 1989. Primary production in the Gernika Estuary during a summer bloom of the dinoflagellate *Peridinium quinquecorne* Abe. Botanica Marina, *32,* 159–165.

Moran, S. B. and R. M. Moore. 1988. Temporal variations in dissolved and particulate aluminum during a spring bloom. Est. Coast. Shelf Sci., *27,* 205–215.

NOAA. 1982. Tidal Current Tables 1983. Pacific Coast of North America and Asia, Rockville, MD, 270 pp.

Officer, C. B. 1977. Longitudinal circulation and mixing relations in estuaries, *in* Estuaries, Geophysics, and the Environment, Washington, D. C., National Academy of Sciences, 13–21.

Paerl, H. H. 1988. Nuisance phytoplankton blooms in coastal, estuarine, and inland waters. Limnol. Oceanogr., *33,* 823–847.

Peterson, D. H., R. E. Smith, S. W. Hager, D. D. Harmon, R. E. Herndon and L. E. Schemel. 1985. Interannual variability in dissolved inorganic nutrients in Northern San Francisco Bay Estuary. Hydrobiologia, *129,* 37–58.

Peterson, W. T. 1986. The effects of seasonal variations in stratification on plankton dynamics in Long Island Sound, *in* Tidal Mixing and Plankton Dynamics, M. J. Bowman, C. M. Yentsch and W. T. Peterson, eds., New York, Springer-Verlag, 297–320.

Platt, T., K. L. Denman and A. D. Jassby. 1977. Modeling the productivity of phytoplankton, *in* The Sea: Ideas and Observations on Programs in the Study of the Seas, E. D. Goldberg, ed., New York, Wiley, 807–856.

Powell, T. M., J. E. Cloern and L. M. Huzzey. 1989. Spatial and temporal variability in South San Francisco Bay. I. Horizontal distributions of salinity, suspended sediments, and phytoplankton biomass and productivity. Est. Coast. Shelf Sci., *28,* 583–597.

Powell, T. M., J. E. Cloern and R. A. Walters. 1986. Phytoplankton spatial distribution in South San Francisco Bay—mesoscale and small-scale variability, *in* Estuarine Variability, D. A. Wolfe, ed., New York, Academic, 369–383.

Riebesell, U. 1989. Comparison of sinking and sedimentation rate measurements in a diatom winter/spring bloom. Mar. Ecol. Progr. Ser., *54,* 109–119.

Sakamoto, M. and T. Tanaka. 1989. Phosphorus dynamics associated with phytoplankton blooms in eutrophic Mikawa Bay, Japan. Mar. Biol., *101,* 265–271.

Simpson, J. H., J. Brown, J. P. Matthews and G. Allen. 1990. Tidal straining, density currents and stirring in the control of estuarine stratification. Estuaries, *13,* 125–132.

Sinclair, M. 1978. Summer phytoplankton variability in the lower St. Lawrence estuary. J. Fish. Res. Bd. Can., *35,* 1171–1185.

Sinclair, M., D. V. Subba Rao and R. Couture. 1981. Phytoplankton temporal distributions in estuaries. Oceanol. Acta., *4,* 239–246.

Strathmann, R. R. 1967. Estimating the organic carbon content of phytoplankton from cell volume or plasma volume. Limnol. Oceanogr., *12,* 411–418.

Strickland, J. D. H. and T. R. Parsons. 1972. A practical handbook of seawater analysis. Bull. Fish. Res. Bd. Can., *167,* 310 pp.

Turner, S. M., G. Malin, P. S. Liss, D. S. Harbour and P. M. Holligan. 1988. The seasonal variation of dimethyl sulfide and dimethyl sulfoniopropionate concentrations in nearshore waters. Limnol. Oceanogr., *33,* 364–375.

Underdal, B., O. M. Skulberg, E. Dahl and T. Aune. 1989. Disastrous bloom of *Chrysochromulina polylepsis* (Prymnesiophyceae) in Norwegian coastal waters 1988—mortality in marine biota. Ambio, *18,* 265–270.

Wienke, S. M. and J. E. Cloern. 1987. The phytoplankton component of seston in San Francisco Bay. Neth. J. Sea Res., *21,* 25–33.

Wienke, S. M., B. E. Cole and J. E. Cloern. 1990. Plankton Studies in San Francisco Bay, California. XI. Chlorophyll distributions and hydrographic properties of San Francisco Bay, 1989–1990. U.S. Geol. Survey Open-File Rept., 90–562.

Winter, D. F., K. Banse and G. C. Anderson. 1975. The dynamics of phytoplankton blooms in Puget Sound, a fjord in the Northwestern United States. Mar. Biol., *29,* 139–176.

Wong, R. L. J. and J. E. Cloern. 1982. Plankton Studies in San Francisco Bay. IV. Phytoplankton abundance and species composition, January 1980–February 1981. U.S. Geol. Survey Open-File Rept., 82–443.

Received: *13 August, 1990;* revised: *29 January, 1991.*